Hindawi
Journal of Chemistry
Volume 2021, Article ID 3416092, 12 pages
https://doi.org/10.1155/2021/3416092

Research Article

Expired Chicken Egg-White Extract's Adsorption Behavior As a Corrosion Inhibitor for Carbon Steel in 1M HCl

Esseddik Elqars,[1] **Mohamed Guennoun**,[1] **Aicha Ouarhach**,[2] **Noufissa Sqalli Houssini**,[1] **Mohammed Elhafdi**,[1] **Abdelhafid Essadki**,[1] **Mohamed Ait chaoui**,[3] **and Taibi Nbigui**[1]

[1]*Laboratoire d'ingénierie des Procédés et d'environnement (LIPE), Université Hassan II, Ecole supérieure de Technologies, BP.8012 Oasis, Casablanca, Morocco*
[2]*Laboratoire de Chimie Appliquée, Département de Chimie, Faculté Des Sciences Semlalia, Université Cadi Ayyad Marrakech, Morocco*
[3]*Laboratory Materials Thematic Research Center the Ben M'sik Faculty of sciences, Hassan II University Casablanca, Morocco*

Correspondence should be addressed to Esseddik Elqars; s.elqars@gmail.com

Received 5 May 2021; Revised 3 July 2021; Accepted 17 August 2021; Published 10 September 2021

Academic Editor: Ajaya Kumar Singh

The inhibitory activity of the expired egg-white carbon steel (CS) extract in HCl solution was studied in this article. The extract was examined using FT-IR, and the surface was examined using a scanning electron microscope (SEM) and energy-dispersive X-ray analysis (EDX). Weight loss techniques at various temperatures were used to examine corrosion investigations (298, 308, 318, and 328 K), concentrations (100, 200, 400, and 800 mg. L^{-1}) of extracts, and electrochemical measurements (potentiodynamic polarization (PDP) and impedance spectroscopy (EIS) at 25°C and different concentrations. *Results*. Results obtained through EIS demonstrated a maximal inhibition efficiency of 90% at an inhibitor concentration of 800 mg. L^{-1}. Moreover, the findings of the potentiodynamic polarization indicated that egg-white extract was a mixed type of inhibitor and slowed down both cathodic and anodic reactions. For weight loss analysis, an inhibitory potency (89, 83, 77, and 71%) at various temperatures (298, 308, 318, and 328 K) was demonstrated, respectively. It indicates that the temperature rise contributes to a decrease in the resistance of the carbon steel. The adsorption of the expired egg-white extract was spontaneous with physisorption and chemisorption according to the Langmuir isotherm model, according to adsorption isotherm studies.

1. Introduction

The corrosion of carbon steel in acidic environments has become a fundamental and industrial problem because of the strong interest of scientists and engineers around the world [1]. The comprehensive use of structural and machinery building purposes renders carbon steel a metallic alloy vulnerable to corrosion degradation [2]. It is further exacerbated by its attractive mechanical and physical qualities, recyclability expense, and availability [3]. Mineral acid is often used in industry to chemically clean carbon steel, stainless steel, titanium, copper, and other alloys [4, 5]. Under these conditions, the choice of inhibitor or inhibitor formulation will depend on the corrosion system involved, especially the nature of the acid, the presence of dissolved organic or inorganic compounds, as well as the temperature, etc. [6, 7]. As corrosion inhibitors, the development of organic extracts has exceeded a certain level; currently, they are the first choice for inhibitors. The inhibitory action of these organic compounds is due to the development of a more or less continuous barrier that inhibits the solution for accessing the metal (or via adsorption) [8–10]. The organic compounds used as inhibitors must have at least one heteroatom working as an active center for their fixation on the metal such as nitrogen (amines, amides, imidazolines, and triazoles), oxygen (acetylenic alcohols, carboxylates, and oxadiazoles), sulfur (thiourea derivative, mercaptans, sulfoxides, and thiazoles), or phosphorus (phosphonates); one

limitation in the application of these products may be the increase in temperature as organic molecules are often unstable at high temperatures [11–13]. Amino acids are effective and environment-friendly corrosion inhibitors that have been extensively researched in experiments and theory under various conditions. Almost all of these amino acids have been tested in acidic solutions against iron corrosion [14–16].

Inhibitors have the originality of being the only means of intervention from the corrosive medium, which makes them an easy and inexpensive method of corrosion control, provided that the products used are of moderate cost [17–19]. In recent years, various studies have centered on reducing the harmful effects of human life on the earth and its potential to sustain life [20, 21]. Thus, there is increasing interest in biodegradable chemistry as there is a demand for innovative ecologically friendly products and biodegradable natural inhibitors from plant or animal origin with a lower concentration to provide greater efficacy [22, 23].

Currently, many types of research are focussing on corrosion inhibition by organic extracts that give a good efficiency such as corrosion inhibition in *Swertia chirata* extract in an acid environment (0.5 M H_2SO_4) [24], *Thevetia peruviana* (Kaner) flower extract (TPFE) [25], leaf extract of *Arbutus unedo* L. [26], *Crotalaria pallida* leaf extracts [27], which were tested for mild steel, in 1M HCl. In our work, we have chosen the expired chicken egg, especially the white part, because the yellow part contains just lipids and the other contains of organic and mineral elements; for this reason, we have chosen the white part [28–31]. Expired egg white, which is available all over the world and is less expensive as an organic (animal origin) corrosion inhibitor for carbon steel in a 1M HCl solution, has a 90% effectiveness at 298 K; we examined weight loss (WL) and electrochemical tests such as potentiodynamic polarization (PDP) curves, electrochemical impedance spectroscopy (EIS), and SEM and EDX to assess the inhibitor efficacy. The isotherm and thermodynamic adsorption characteristics, as well as the adsorption mechanism, are all investigated.

2. Experimental Procedures

2.1. Extraction Procedure. Figure 1 shows the preparation of expired egg-white extract (EEW). The EEW is dried in an oven at 308 K for 120 hours to make the drying completely uniform. Then, the resulting solid was crushed and sieved to obtain a fine powder. Accurate amounts were added to a concentrated 1M HCl solution (37%) to get the total solubility. Then, the whole solution was adjusted with distilled water to finally obtain extract concentrations (0.1, 0.2, 0.4, and 0.8 g/L) in a 1M HCl solution.

2.2. Weight Loss Measurements. The inhibitory effect of the EEW extract was tested on a carbon steel specimen with dimensions of 2.26-1.33-0.30 cm^2 and a chemical composition of 0.63 Cr (percent by weight) and S, 0.35–0.39% C, 0.50–0.80% Mn, Ni, and Mo, 0.015–0.035% S, 0.35–0.39% C, 0.50–0.80 Mn, and 0.40% Si, with the rest being Fe. We repeated each test three times for consistency, and the analytical balance can read up to four decimal places. The carbon steel specimen was polished with 400-, 600-, 800-, and 1200-grade abrasive paper before each experiment. Acetone was used to degrease the surface, which was then rinsed with distilled water. The samples were subsequently submerged in 100 ml of EEW extract at various concentrations. The examination lasted 6 hours. They were weighed again after being washed with distilled water. This investigation was also carried out at various temperatures (298, 308, 318, 328 K).

The rate of corrosion (CR), (θ) surface coverage, and inhibition efficiency (η%) [32, 33] were put to use.

$$CR = \frac{W_0 - W_t}{\text{S.t}},$$

$$\theta = \frac{CR_{\text{int},0} - CR_{inh}}{CR_{\text{int},0}}, \tag{1}$$

$$\eta\% = \frac{CR_{inh,0} - CR_{inh}}{CR_{inh,0}} \times 100,$$

where W_0 and W_t are, respectively, the carbon steel mass values before and after immersion in the corrosive solution (mg). S is the carbon steel surface area (cm^2), t is the corrosion time in (h), CR_{inh} and $CR_{\text{int},0}$ are, respectively, the corrosion rate, with and without inhibitors $g.cm^2h^{-1}$.

2.3. Electrochemical Measurements. An OrigaLys potentiostat was used to make the electrochemical measurements. The Origa Master 5 software controls the system is fitted with a traditional three-electrode setup. The working electrode (WE) was made of carbon steel with a diameter of 0.28 cm^2. The platinum electrode serves as a counter electrode (CE), while the reference electrode is a calomel-saturated (Hg_2Cl_2/Hg) electrode (RE). The electrode potential was automatically adjusted in the range of 300 mV more or less than the E_{corr} at 1 mV/s to evaluate potentiodynamic polarization (PDP) curves. The frequency range for the measurements was 20 kHz to 200 MHz, with a 20 point per decade amplitude. Prior to each test, the working electrode (WE) was polished using abrasive series paper (400, 600, 800, and 1200), and distilled water and acetone were used to monitor the process. All of the trials were carried out at 298 K.

3. Results and Discussion

3.1. FT-IR Spectroscopy Results. The presence of functional groups and heteroatoms is the most crucial item in the adsorption of inhibitor molecules to the iron surface, as seen in the FT-IR spectrum of expired egg-white extract in Figure 2. The existence of various functional groups may be seen in the IR spectra (Figure 2). The wide and strong bands in the range of 3500–3000 cm^{-1} are attributed to the OH/N–H/CH group [34]. The bands observed at 1650 cm^{-1} correspond to the C=O stretch group, and the absorption bands at 1550 cm^{-1} correspond to N–H/C=*C* stretch

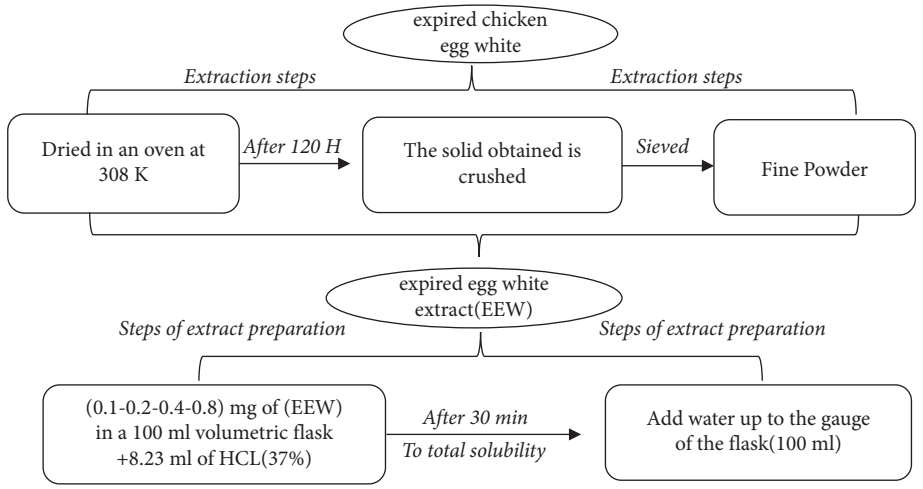

Figure 1: Extraction flowchart of EEW.

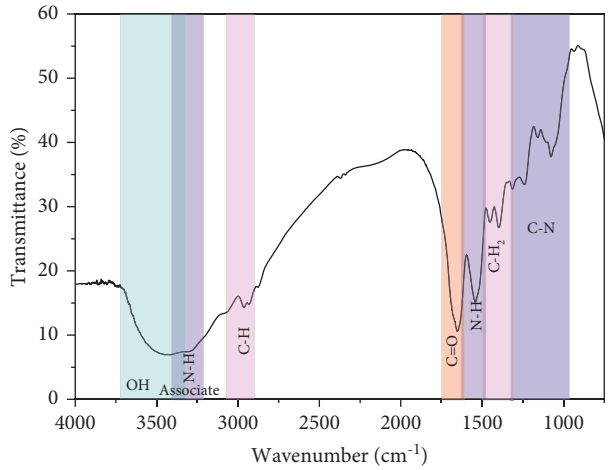

Figure 2: The EEW aqueous extract's infrared spectrum.

(aromatic nucleus) [35]. The C–H2 bands are observed around 1460 cm^{-1} and 1396 cm^{-1}.The bands between 1360 and 1080 cm^{-1} are assigned to the C-N bands [36].

3.2. WL Measurements. To get a better understanding of how corrosion is inhibited. The weight loss technique was used to examine the effect of different doses on the inhibitory potential of EEW at 298, 308, 318, and 328 K. Table 1 and Figure 3 demonstrate the corrosion rate (CR) and inhibition efficiency (η%); the efficacy of the inhibition rises as the inhibitor concentration increases, suggesting an increase in surface coverage and blocking the activation activity on the carbon steel surface. Furthermore, these findings revealed that, at all temperatures examined, the inhibition was efficient, the EEW lowered the CR values, and as the temperature of the solution grew, the percent values for EW dropped. This lowered corrosion rate with rising temperature may be explained further by a preexponential factor, which results from decreased desorption of inhibitor species from the carbon steel surface. The influence of temperature on the ΔH_{ads} and ΔS_{ads} of the corrosion process may be assessed.

3.3. Adsorption Isotherm and Thermodynamic Parameters. Adsorption isotherm investigations reveal the process by which inhibitors bind to metal surfaces. Adjusting the corrosion rate CR and the degree of inhibitor surface coverage yielded the isotherm adsorption model that best reflects the adsorption of EEW on carbon steel in a 1 M HCl medium. Different isotherm adsorption models are used (Langmuir, Temkin, El-Awady's, Freundlich, and Flory–Huggins) expressed in the linear form:

Langmuir adsorption isotherm [37]:

$$\frac{C_{inh}}{\theta} = \frac{1}{K_{a\ ds}} + C_{inh}. \quad (2)$$

El-Awady's thermodynamic/kinetic adsorption isotherm model [38, 39]:

Table 1: Carbon steel corrosion weight loss results in a 1 M HCl solution in the absence and presence of different inhibitor concentrations and EEW temperatures from 298 to 328 K.

	298 K			308 K			318 K			328 K		
C_{inh} $g.l^{-1}$	CR g.cm$^{-2}h^{-1}10^{-3}$	θ	η (%)	CR g.cm$^{-2}h^{-1}10^{-3}$	θ	η (%)	CR g.cm$^{-2}h^{-1}10^{-3}$	θ	η (%)	CR g.cm$^{-2}h^{-1}10^{-3}$	θ	η (%)
Blank	3.34			4.29			5.09			6.31		
0.1	0.99	0.71	70	1.46	0.66	66	2.13	0.58	58	2.94	0.53	53
0.2	0.75	0.78	78	1.14	0.73	73	1.67	0.67	67	2.46	0.61	61
0.4	0.59	0.82	82	0.99	0.77	77	1.48	0.71	71	2.26	0.64	64
0.8	0.38	0.89	89	0.72	0.83	83	1.22	0.76	76	1.82	0.71	71

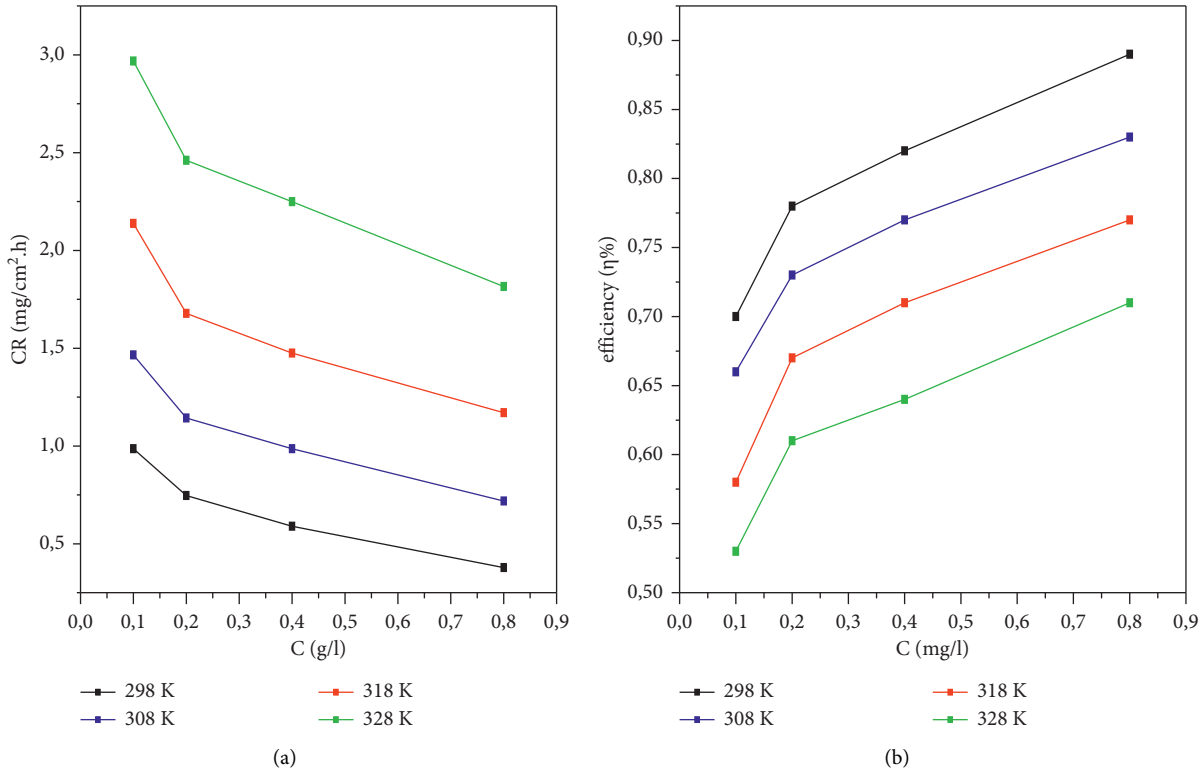

Figure 3: (a) Inhibition efficiency and (b) corrosion rate with the effect of temperature for different concentrations of the extract EEW.

$$\log\left(\frac{\theta}{1-\theta}\right) = y.\ \log C_{inh} + \log K. \quad (3)$$

Temkin adsorption isotherm model [40]:

$$\theta = \ln C_R + K_{a\ ds}. \quad (4)$$

Freundlich adsorption isotherm [41]:

$$\log \theta = \log K_{a\ ds} + n.\ \log C_{inh}. \quad (5)$$

Flory–Huggins adsorption isotherm [42]:

$$\log\frac{\theta}{CR} = b.\ \log(1-\theta) + \log K_{a\ ds}. \quad (6)$$

This research is to find the R2 correlation coefficient for each isothermal model of Table 2. The best-fitting model was chosen based on the correlation coefficient. In this research, the Langmuir isotherm with a 0.999 corrélation coefficient value provided the greatest match to experimental data. In a hydrochloric acid medium, it explains a superior adsorption mechanism of the EEW extract on carbon steel.

To comprehend the kind of EEW adsorption in the metal/solution contact, the following formula is used to calculate the value of ΔG_{ads}:

$$\Delta G_{a\ ds} = -RT.\ \ln\left(C_{H_2O}.K_{a\ ds}\right), \quad (7)$$

where T is the absolute temperature (K), R is the gas constant, $K_{a\ ds}$ is the adsorption equilibrium constant calculated from the isotherm, 8.314 JK^{-1}mol^{-1}, and C_{H_2O} is the value of the concentration of water in the solution ($1000 g.l^{-1}$)[43, 44].

The negative values of $\Delta G_{a\ ds}$ obtained as in Table.3, according to Figure 4, guarantee the adsorption

Table 2: Correlation coefficient values for the various adsorption isotherms considered.

Temperature (k)	Langmuir R^2	El-Awady's R^2	Temkin R^2	Freundlich R^2	Flory–Huggins R^2
298	0.9994	0.9869	0.9775	0.9903	0.9799
308	0.9992	0.9855	0.9864	0.9783	0.9798
318	0.9994	0.9835	0.9904	0.9617	0.9820
328	0.9986	0.9800	0.9933	0.9712	0.9731

Table 3: Thermodynamic characteristics for 1 M HCl adsorption on carbon steel at temperatures of 298; 308; 318; and 328 K.

T(K)	$K_{a\ ds}(g.L^{-1})$	$\Delta G(\text{kJ.mol}^{-1})$
298	24.58	−25.05
308	22.84	−25.70
318	18.55	−25.98
328	15.26	−26.27

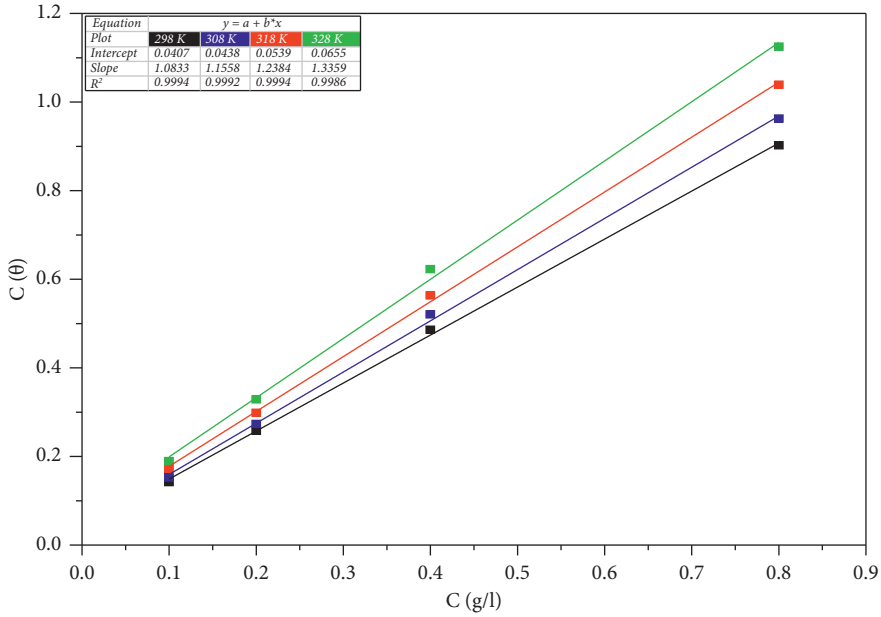

Figure 4: Langmuir adsorption isotherm model for EEW on the carbon steel surface at temperatures from 298 to 328 K.

mechanism's spontaneity and stability on the carbon steel surface. The $\Delta G_{a\ ds}$ values are between −25 and −26 kJ.mol^{-1}, which are lower than −20 kJ.mol^{-1} and higher than −40 kJ.mol^{-1}, indicating that adsorption of inhibitor molecules on the carbon steel surface includes both physisorption and chemisorption [45].

The corrosion thermodynamic parameters were used to further analyze the adsorption behavior of EEW on the carbon steel surface. Arrhenius and transition state equations were used to calculate activation energy (Ea), entropy (ΔS_a), and activation enthalpy (ΔH_a).

The activation energy (Ea) was calculated using the following equation [46]:

$$\log(CR) = -\frac{E_a}{2.303RT} + \log\lambda, \quad (8)$$

where R is the universal gas constant, T is the absolute temperature (K), and is the frequency factor.

The connection between Log (CR) and 1000/T in 1 M HCl without and with the EW inhibitor produces straight lines with slopes of $E_a/2.303RT$, as illustrated in Figure 5. The estimated values of the apparent activation energy using equation (8) are given in Table 4.

The equation of transition states is

$$\log\left(\frac{CR}{T}\right) = -\frac{\Delta H_{a\ ds}}{2.303R}\left(\frac{1}{T}\right) + \left[\frac{\Delta S_{a\ ds}}{2.303R} + \log\left(\frac{R}{N_A.h}\right)\right], \quad (9)$$

where $(N_A = 6.023 \times 10^{23})$ is Avogadro's number, $(h = 6.62607 \times 10^{-34})$is Planck's constant, $\Delta H_{a\ ds}$ is the enthalpy, and $\Delta S_{a\ ds}$is the entropy of adsorption. Figure 6 displays the plot of $\log(CR/T)$ versus which will give a straight line, with a slope of $\Delta H_{a\ ds}/2.303R$ and an intercept of$[\Delta S_{a\ ds}/2.303R + \log(R/N_A.h)]$. Thus, giving the values of $\Delta S_{a\ ds}$ and $\Delta H_{a\ ds}$, results are shown in Table 4.

The values $\Delta H_{a\ ds}$ are positive, indicating an endothermic corrosion process [48]. The values of E_a and

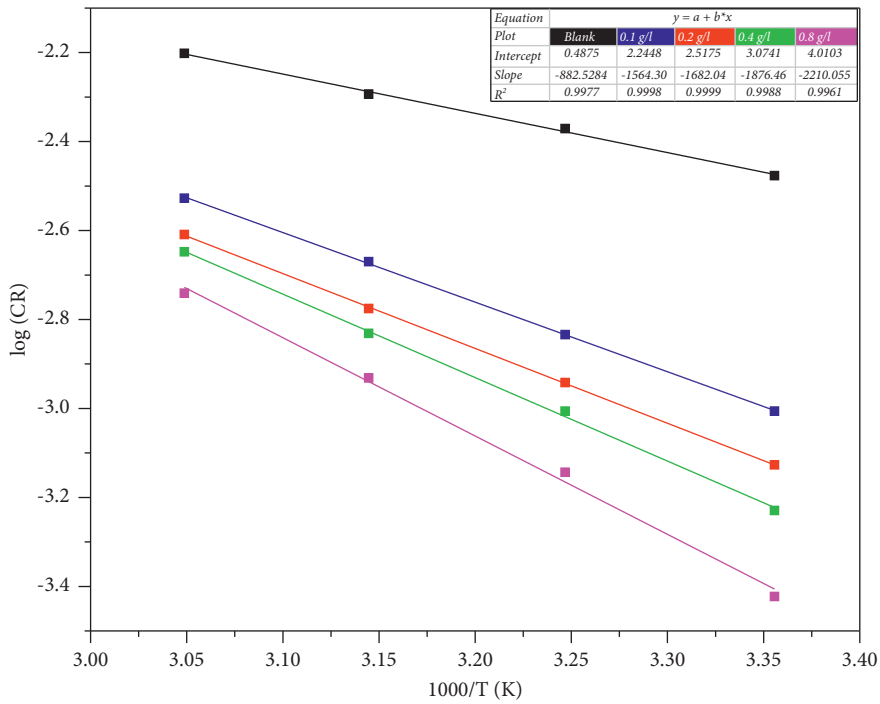

Figure 5: Carbon steel corrosion in 1 M HCl in the absence and presence of EW and the Arrhenius plot of log (CR) versus 1000/T. The activation entropy (ΔS_{ads}) and activation enthalpy (ΔH_{ads}) are shown, and Arrhenius was used to achieve the results [47].

Table 4: Values for E_a, $\Delta H_{a\,ds}$, and $\Delta S_{a\,ds}$ in the absence of inhibitors and in the presence of inhibitors of varying doses.

C_{inh} ($g.L^{-1}$)	E_a (kJ.mol^{-1})	$\Delta H_{a\,ds}$ (kJ.mol^{-1})	$E_a - \Delta H_{a\,ds}$	$\Delta S_{a\,ds}$ (J.mol^{-1}.K^{-1})
Blank	16.90	14.30	2.60	−244.34
0.1	29.95	27.35	2.60	−210.69
0.2	32.21	29.61	2.60	−205.47
0.4	35.93	33.33	2.60	−194.81
0.8	42.32	39.72	2.60	−176.88

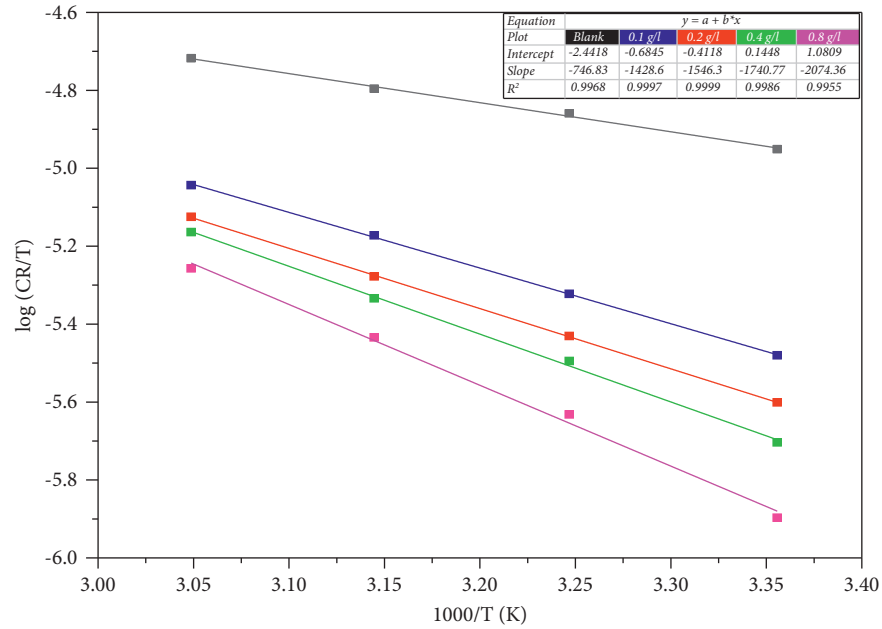

Figure 6: Transition state plot of log (CR/T) vs. 1000/T for carbon steel corrosion in 1 M HCl in the absence and presence of EEW.

$\Delta H_{a\ ds}$have increased in the presence of an inhibitor EEW due to the increased energy barrier of the corrosion reaction occurring at the metal surface. Because the corrosion process is a unimolecular reaction, the mean value of the difference $E_a - \Delta H_{a\ ds}$ is 2.60 kJ/mol, which is identical to the mean value of the product RT described by the following equation: $E_a - \Delta H_{a\ ds} = RT$[49].

The activation entropy's high and negative values indicate that the complex activated in the rate-determining step is an association rather than a dissociation phase, implying that there is a decrease in disorder throughout the transition from reactants to activated complexes [50].

3.4. Electrochemical Studies

3.4.1. PDP Measurements. Carbon steel polarization curves in a 1M HCl solution at 298 K were also produced in the absence and presence of EEW inhibitors of various doses. The entire behavior of the steel/acid/inhibitor system is depicted in Figure 7. Table 5 illustrates the inhibition efficacy of different doses of inhibitor in 1M HCl for corrosion current densities (Icorr), corrosion potential (Ecorr), Tafel slope (βa) and (βc), and EI (%). Equation (10) defines the corrosion inhibiting effectiveness (%):

$$\eta_{P\ DP} = \frac{i_{\text{coor}} - i_{inh}}{i_{\text{coor}}} \times 100. \tag{10}$$

The current densities without and with inhibitor, as calculated by extrapolation of the Tafel lines, are I_{corr} and I_{inh}, respectively [51, 52].

The inhibitory capacity of the inhibitor was studied using a polarization test, and the results are shown in Figure 7; it can be seen that by the successive addition of an egg-white extract to the 1 M HCl medium, in the presence of the EEW, the corrosion potential is somewhat pushed towards the cathode branch, with a fluctuation in the values of β_a and β_c. This indicates that the presence of inhibitors in an acidic environment slowed both carbon steel dissolving and hydrogen reduction [53, 54]. In comparison to the blank, there is no significant change in the corrosive potential readings. The E_{corr} is displacement is less than 85 mV, indicating that it is a mixed-character inhibitor [55, 56]. As the corrosion concentration of the inhibitors increases, the corrosion current density values decrease [57] according to the data given in Table 6. These results can be ascribed to the adsorption of EEW on the carbon steel surface, which reduces the active site's surface area and can function as a corrosion barrier [58, 59]. It should also be noted that a good inhibition efficiency was observed in the presence of EEW (89%) at a concentration of 800 mg. L^{-1}.

3.4.2. Impedance Spectroscopy Electrochemical. Electrochemical impedance spectroscopy is widely and effectively applied in global corrosion and protection processes, addressing the use of electrochemical impedance measurements to investigate the inhibitory mechanism; it seems that this technique is particularly adapted to determine the mode of action of inhibitors; it allows evaluating

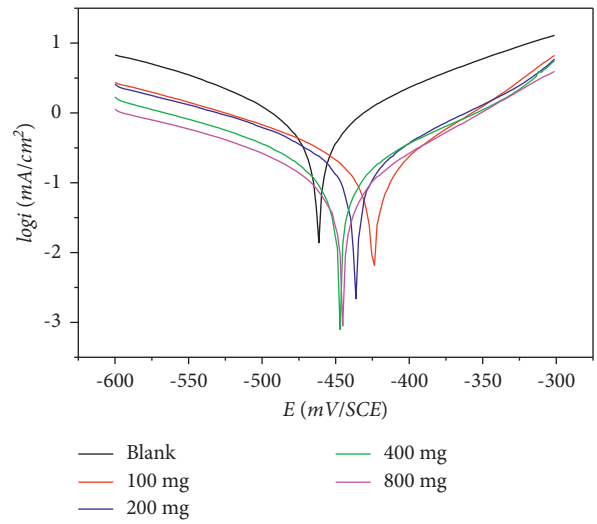

Figure 7: Carbon steel polarization curve in 1M HCl without and with the addition of EEW at 298 K.

the dielectric characteristics of the film formed and to follow their evolution according to many parameters [60, 61]. It also makes it possible to explain the chemical or electrochemical processes developing through the films. In this study of corrosion inhibition of carbon steel in 1 M HCL acid media at 298 K, the impedance of the Nyquist and Bode diagrams is presented in Figures 8(a)and 8(b).

Figure 8(a) shows the equivalent circuit, rather than using capacitors, uses stationary-phase elements (CPE) to provide a variety of heterogeneities suitable for corrosion electrodes, such as deficient polishing, grain boundary, surface contaminants, and surface roughness [62]. We utilized the parameters (n and Y_0) of our test to construct a mathematical model since the impedance of carbon steel is frequency dependent.

$$Z_{CPE} = \frac{1}{Y_0 (j\omega)^n}, \tag{11}$$

where Y_0 denotes the CPE constant, j is an imaginary number and $j^2 = -1$, ω represents the angular frequency in rad^{-1} and $\omega = 2\pi f$, and n is a measure of the roughness of the carbon steel surface; $0 \le n \le 1$ [63]. In addition, this is due to a variety of factors, including electrode roughness, dielectric constant, and surface heterogeneity; in our research, the n values are in a range of $0.981 < n < 0.996$, indicating that inhibitors have no effect on the mechanism of corrosion and that the electron transfer reaction regulates the corrosion process both in the absence and presence of inhibitors [64]. The following equation was used to determine the double-layer amplitude (C_{dl}):

$$C_{dl} = \frac{1}{2\pi f_{\max} R_p}, \tag{12}$$

where $f_{\max}$ is the maximum frequency of the imaginary component of the impedance and R_p is the charge transfer resistance; it is evident from Table 5 that the C_{dl} values decreased in the presence of the inhibitor, owing to an increase in the thickness of the protective layer on the

Table 5: Electrochemical parameters of impedance for carbon-steel in 1M HCL, without and with EEW at 298 K.

$C_{inh}\,(mg.l^{-1})$	$R_s\,(\Omega.cm^2)$	$R_p\,(\Omega.cm^2)$	n	$C_{dl}\,(\mu F/cm^2)$	$\eta_{EIS}\,(\%)$
Blank	1.1843	27.97	0.996	507.19	—
100	1.6922	95.26	0.994	132.72	71
200	2.7586	128.13	0.989	124.13	78
400	1.7158	184.39	0.992	108.65	85
800	1.9662	271.77	0.996	82.718	90

Table 6: Potentiodynamic polarization results for carbon-steel in 1M HCL, without and with EEW at 298 K.

$C_{inh}\,(g.l^{-1})$	$-E_{coor}\,(mv/SCE)$	$i_{coor}\,(\mu A/cm^2)$	$\beta_a\,(mv/déc)$	$-\beta_c\,(mv/déc)$	$\eta_{PDP}\,(\%)$
Blank	461.8	735.5	121.0	129.5	—
100	424.4	210.9	89.0	148.3	71
200	436.4	174.4	98.0	114.3	76
400	447.5	135.2	106.3	122.4	82
800	445.2	80.4	85.3	106.4	89

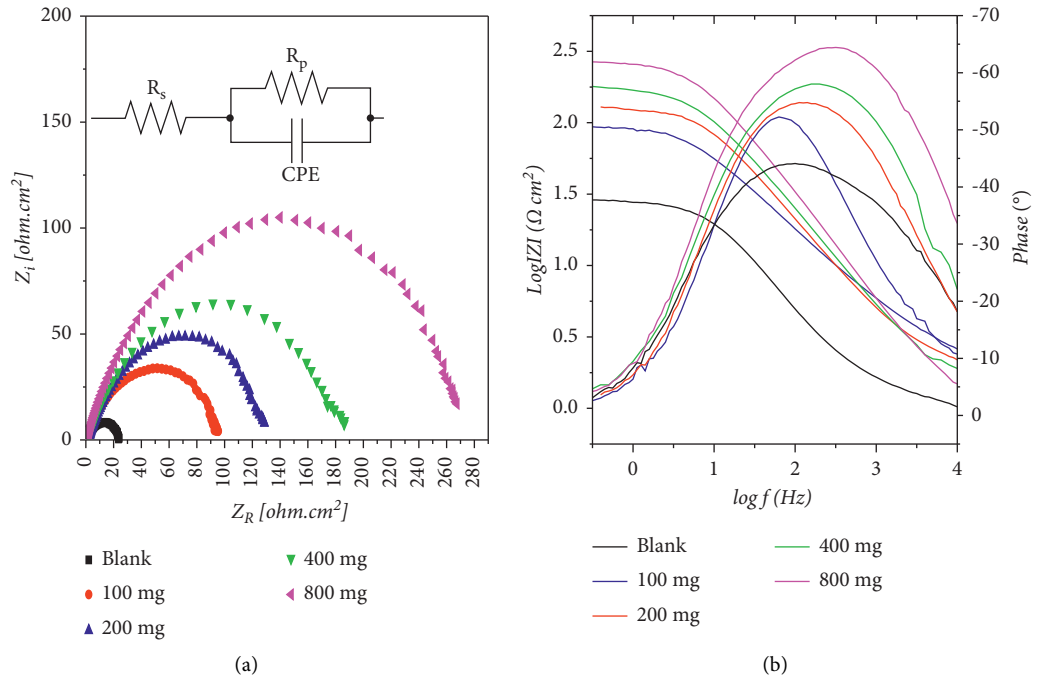

Figure 8: (a) Nyquist plots in the absence and presence of a different concentration of EEW, equivalent circuit used, and (b) bode-phase angle plots in the absence and presence of a different concentration of EEW.

electrode surface in the presence of an inhibitor [65]; in other words, the decrease in C_{dl} values is attributed to the progressive replacement of water molecules adsorbed on the metal surface by larger water molecules [66].

In this work, we looked at the efficacy of inhibition $\eta_{EIS}\,(\%)$ using the following equation [67]:

$$\eta_{EIS} = \frac{R_s - R_p}{R_2} \times 100, \tag{13}$$

where R_p^{inh} and R_p^{corr} are the charge transfer resistance values with and without EEG, respectively; furthermore, it is clear from Table 5 that the values of Rp increase significantly with the increase of the inhibitor concentration in the acid solution, the polarization resistance (Rp) is inversely related to the corrosion rate, and the creation of an insulating protective coating at the metal/solution contact is responsible for the increase in Rp values [68]. This gives a maximum inhibitor concentration efficiency of 90% at 800 mg/L of EEW; these findings support the hypothesis that EEW works via adsorption at the metal/solution contact. Figure 8(b) show the impedance data in Bode diagrams of impedance size ($|Z|$) and full-frequency angle of phase for the C-steel electrode obtained at various inhibitor doses; furthermore,

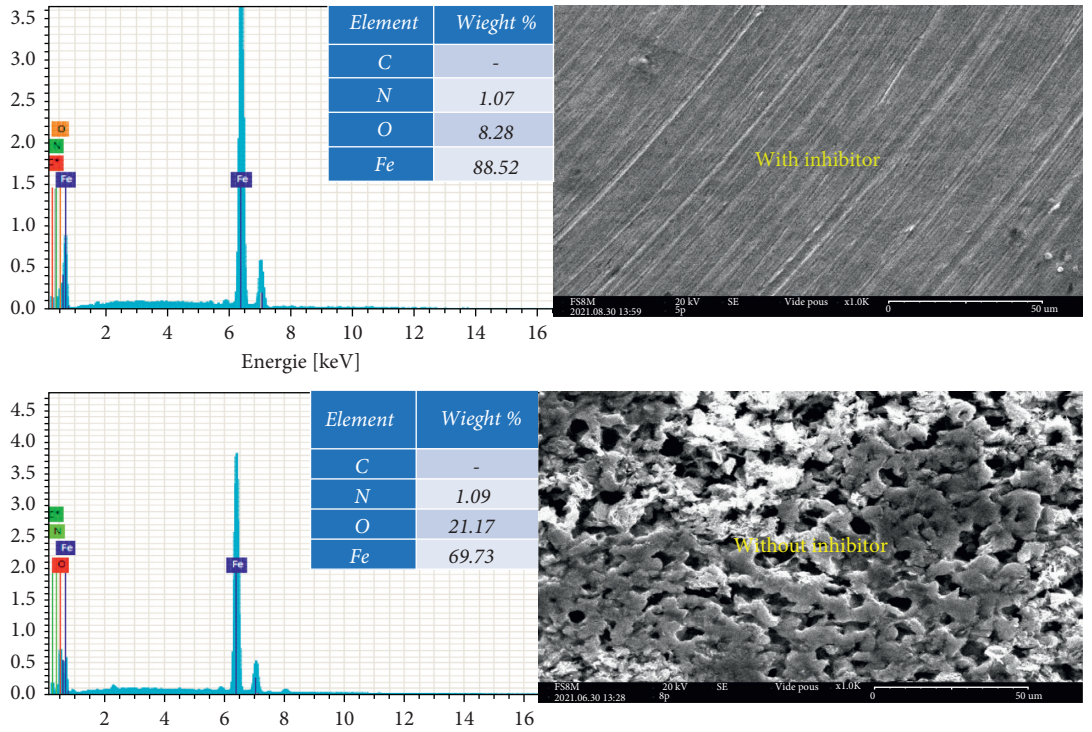

FIGURE 9: SEM image of the surface with an inhibitor and without an inhibitor (EW) of carbon steel with EDX spectra corresponding to each image.

when the concentration of inhibitors increases, the angle of phase increases up to 65° in comparison to the noninhibited system, indicating an improvement in inhibition performance via EEG adsorption on the CS surface [69, 70]. This may explain the efficacy in the current research due to the presence of these features in the EEG, as well as delocalized electron density in the majority of the molecular structure. In the same way, the higher efficiency of EEG, in contrast to *Lilium brownii* leaf extract [71], camphor leaf extract [72], and *Tamarindus indica* extract [73], can be explained by that the EEG contains many electron sources such as oxygen atoms, nitrogen atom, and hydroxy group, confirming the benefit of using EEG as a corrosion inhibitor.

3.4.3. EDX Spectra and Scanning Electron Microscopy (SEM) Surface Analysis. Figure 9 shows the surface morphology of carbon steel during 12 hours of immersion with and without an inhibitor in a 1M HCl solution at 298 K. The SEM analysis shows the surface of the steel with and without an inhibitor so that the surface with an inhibitor is at the energy 20 KV. The surface morphology was severely degraded by exposing the specimen to 1 M HCl, as seen in Figure 9 (blank). After immersion in an acidic solution containing 800 mg, the surface of the specimen was smoother and revealed fewer pits. When inhibitor molecules engage with the corroding surface of CS in the acid solution, a protective barrier layer is formed, resulting in the smoothness of the inhibited CS surface [74–76].

4. Conclusions

The inhibition behavior of the expired egg-white extract (EEW) in 1M HCl was examined using weight loss, electrochemical study, and SEM with EDX:

Potentiodynamic polarization (PDP) studies show that this natural product is a mixed-type inhibitor and acts as an adsorptive inhibitor

Increasing the inhibitor concentration up to 800 mg/L at 298 K, the inhibition efficiency increases to 89% for (PDP) and 90% for (EIS)

The site electrochemical impedance spectroscopy indicated that the ECP, with increasing inhibitor concentrations, and the charge transfer resistance of the electrical double layer dropped and the charge transfer resistance rose

The effect of temperature showed that extract adsorption occurs by physical and chemical adsorption and follows the Langmuir isotherm

Scanning electron microscopy reveals the development of a protective layer on the metal surface

Data Availability

The data used to support the findings of this study are available from the author upon request.

Conflicts of Interest

All of the authors have no affiliation with any organization with a direct or indirect financial interest in the subject matter discussed in the manuscript.

References

[1] Q. Wang, B. Tan, H. Bao et al., "Evaluation of Ficus tikoua leaves extract as an eco-friendly corrosion inhibitor for carbon steel in HCl media," *Bioelectrochemistry*, vol. 128, pp. 49–55, 2019.

[2] M. Mobin, M. Basik, and J. Aslam, "Pineapple stem extract (Bromelain) as an environmental friendly novel corrosion inhibitor for low carbon steel in 1 M HCl," *Measurement*, vol. 134, pp. 595–605, 2019.

[3] I. Ahamad, R. Prasad, and M. A. Quraishi, "Inhibition of mild steel corrosion in acid solution by Pheniramine drug: experimental and theoretical study," *Corrosion Science*, vol. 52, no. 9, pp. 3033–3041, 2010.

[4] F. Bouhlal, N. Labjar, F. Abdoun et al., "Electrochemical and thermodynamic investigation on corrosion inhibition of C38 steel in 1M hydrochloric acid using the hydro-alcoholic extract of used coffee grounds," *International Journal of Corrosion*, vol. 2020, Article ID 4045802, 14 pages, 2020.

[5] B. Chugh, S. Thakur, B. Pani et al., "Investigation of phenol-formaldehyde resins as corrosion impeding agent in acid solution," *Journal of Molecular Liquids*, vol. 330, Article ID 115649, 2021.

[6] I.-I. N. Etim, J. Dong, J. Wei et al., "Effect of organic silicon quaternary ammonium salts on mitigating corrosion of reinforced steel induced by SRB in mild alkaline simulated concrete pore solution," *Journal of Materials Science & Technology*, vol. 64, pp. 126–140, 2021.

[7] B. Chugh, A. K. Singh, S. Thakur et al., "An exploration about the interaction of mild steel with hydrochloric acid in the presence of N-(Benzo[d]thiazole-2-yl)-1-phenylethan-1-imines," *Journal of Physical Chemistry C*, vol. 123, no. 37, pp. 22897–22917, 2019.

[8] Z. Zhang, H. Ba, and Z. Wu, "Sustainable corrosion inhibitor for steel in simulated concrete pore solution by maize gluten meal extract: electrochemical and adsorption behavior studies," *Construction and Building Materials*, vol. 227, Article ID 117080, 2019.

[9] K. Hanini, B. Merzoug, S. Boudiba, I. Selatnia, H. Laouer, and S. Akkal, "Influence of different polyphenol extracts of Taxus baccata on the corrosion process and their effect as additives in electrodeposition," *Sustainable Chemistry and Pharmacy*, vol. 14, Article ID 100189, 2019.

[10] A. Singh, X. Dayu, E. Ituen et al., "Tobacco extracted from the discarded cigarettes as an inhibitor of copper and zinc corrosion in an ASTM standard D1141-98(2013) artificial seawater solution," *Journal of Materials Research and Technology*, vol. 9, no. 3, pp. 5161–5173, 2020.

[11] I. Nadi, Z. Belattmania, B. Sabour et al., "Sargassum muticum extract based on alginate biopolymer as a new efficient biological corrosion inhibitor for carbon steel in hydrochloric acid pickling environment: gravimetric, electrochemical and surface studies," *International Journal of Biological Macromolecules*, vol. 141, pp. 137–149, 2019.

[12] M. Boudalia, R. M. Fernández-Domene, M. Tabyaoui, A. Bellaouchou, A. Guenbour, and J. García-Antón, "Green approach to corrosion inhibition of stainless steel in phosphoric acid of Artemesia herba albamedium using plant extract," *Journal of Materials Research and Technology*, vol. 8, no. 6, pp. 5763–5773, 2019.

[13] A. A. Khadom, A. N. Abd, and N. A. Ahmed, "*Xanthium strumarium* leaves extracts as a friendly corrosion inhibitor of low carbon steel in hydrochloric acid: kinetics and mathematical studies," *South African Journal of Chemical Engineering*, vol. 25, pp. 13–21, 2018.

[14] R. Aslam, M. Mobin, Huda, I. B. Obot, and A. H. Alamri, "Ionic liquids derived from α-amino acid ester salts as potent green corrosion inhibitors for mild steel in 1M HCl," *Journal of Molecular Liquids*, vol. 318, Article ID 113982, 2020.

[15] D. Kumar, N. Jain, V. Jain, and B. Rai, "Amino acids as copper corrosion inhibitors: a density functional theory approach," *Applied Surface Science*, vol. 514, Article ID 145905, 2020.

[16] R. Zhao, W. Xu, Q. Yu, and L. Niu, "Synergistic effect of SAMs of S-containing amino acids and surfactant on corrosion inhibition of 316L stainless steel in 0.5 M NaCl solution," *Journal of Molecular Liquids*, vol. 318, Article ID 114322, 2020.

[17] M. Benarioua, A. Mihi, N. Bouzeghaia, and M. Naoun, "Mild steel corrosion inhibition by parsley (Petroselium Sativum) extract in acidic media," *Egyptian Journal of Petroleum*, vol. 28, no. 2, pp. 155–159, 2019.

[18] M. A. Bidi, M. Azadi, and M. Rassouli, "A new green inhibitor for lowering the corrosion rate of carbon steel in 1 M HCl solution: hyalomma tick extract," *Materials Today Communications*, vol. 24, Article ID 100996, 2020.

[19] M. Yang, J. Li, Y. Man, Z. Peng, X. Zhang, and X. Luo, "A novel hollow alumina sphere-based ceramic bonded by in situ mullite whisker framework," *Materials & Design*, vol. 186, Article ID 108334, 2020.

[20] M. R. Mishrif, M. R. Noor El-Din, and E. A. Khamis, "Utilization of ethoxylated pentamine oleamide as new Gemini surfactants for corrosion inhibition effectiveness in 1 M HCl solution," *Egyptian Journal of Petroleum*, vol. 27, no. 4, pp. 1357–1370, 2018.

[21] L. Feng, S. Zhang, Y. Lu, B. Tan, S. Chen, and L. Guo, "Synergistic corrosion inhibition effect of thiazolyl-based ionic liquids between anions and cations for copper in HCl solution," *Applied Surface Science*, vol. 483, pp. 901–911, 2019.

[22] S. Nikpour, M. Ramezanzadeh, G. Bahlakeh, B. Ramezanzadeh, and M. Mahdavian, "Eriobotrya japonica Lindl leaves extract application for effective corrosion mitigation of mild steel in HCl solution: experimental and computational studies," *Construction and Building Materials*, vol. 220, pp. 161–176, 2019.

[23] N. Nava, E. Sosa, J. L. Alamilla, C. Knigth, and A. Contreras, "Field sludge characterization obtained from inner of pipelines," *Corrosion Science*, vol. 51, no. 11, pp. 2652–2656, 2009.

[24] R. Haldhar, D. Prasad, L. T. D. Nguyen et al., "Corrosion inhibition, surface adsorption and computational studies of Swertia chirata extract: a sustainable and green approach," *Materials Chemistry and Physics*, vol. 267, Article ID 124613, 2021.

[25] J. Haque, C. Verma, V. Srivastava, and W. B. W. Nik, "Corrosion inhibition of mild steel in 1M HCl using environmentally benign Thevetia peruviana flower extracts," *Sustainable Chemistry and Pharmacy*, vol. 19, Article ID 100354, 2021.

[26] S. Abdelaziz, M. Benamira, L. Messaadia, Y. Boughoues, H. Lahmar, and A. Boudjerda, "Green corrosion inhibition of mild steel in HCl medium using leaves extract of Arbutus unedo L. plant: an experimental and computational

approach," *Colloids and Surfaces A: Physicochemical and Engineering Aspects*, vol. 619, Article ID 126496, 2021.

[27] A. T. Jeeja Rani, A. Thomas, and A. Joseph, "Inhibition of mild steel corrosion in HCl using aqueous and alcoholic extracts of Crotalaria Pallida - a combination of experimental, simulation and theoretical studies," *Journal of Molecular Liquids*, vol. 334, p. 116515, 2021.

[28] K. Mann and M. Mann, "In-depth analysis of the chicken egg white proteome using an LTQ Orbitrap Velos," *Proteome Science*, vol. 9, no. 1, p. 7, 2011.

[29] T. Ogura, M. Wakayama, Y. Ashino et al., "Effects of feed crops and boiling on chicken egg yolk and white determined by a metabolome analysis," *Food Chemistry*, vol. 327, Article ID 127077, 2020.

[30] W. C. Byrdwell and R. H. Perry, "Liquid chromatography with dual parallel mass spectrometry and 31P nuclear magnetic resonance spectroscopy for analysis of sphingomyelin and dihydrosphingomyelin," *Journal of Chromatography A*, vol. 1133, no. 1-2, pp. 149–171, 2006.

[31] Y.-Q. Liu, C. R. Davis, S. T. Schmaelzle, T. Rocheford, M. E. Cook, and S. A. Tanumihardjo, "β-Cryptoxanthin biofortified maize (Zea mays) increases β-cryptoxanthin concentration and enhances the color of chicken egg yolk „" *Poultry Science*, vol. 91, no. 2, pp. 432–438, 2012.

[32] A. Addoun, S. Bouyegh, M. Dahmane, O. Ferroukhi, and M. Trari, "Thermodynamic investigation on the adhesion and corrosion inhibition properties of a non-steroidal anti-inflammatory drug in HCl electrolyte applied on mild steel material," *Materials Today Communications*, vol. 21, Article ID 100720, 2019.

[33] P. Matheswaran and A. K. Ramasamy, "Influence of benzotriazole on corrosion inhibition of mild steel in citric acid medium," *E-Journal of Chemistry*, vol. 7, no. 3, pp. 1090–1094, 2010.

[34] S. Peshoria and A. K. Narula, "One-pot synthesis of porphyrin@polypyrrole hybrid and its application as an electrochemical sensor," *Materials Science and Engineering: B*, vol. 229, pp. 53–58, 2018.

[35] X. Peng, G. Zhang, Y. Liao, and D. Gong, "Inhibitory kinetics and mechanism of kaempferol on α-glucosidase," *Food Chemistry*, vol. 190, pp. 207–215, 2016.

[36] P. Kannan, P. Jithinraj, and M. Natesan, "Multiphasic inhibition of mild steel corrosion in H 2 S gas environment," *Arabian Journal of Chemistry*, vol. 11, no. 3, pp. 388–404, 2018.

[37] M. Gao, J. Zhang, Q. Liu, J. Li, R. Zhang, and G. Chen, "Effect of the alkyl chain of quaternary ammonium cationic surfactants on corrosion inhibition in hydrochloric acid solution," *Comptes Rendus Chimie*, vol. 22, no. 5, pp. 355–362, 2019.

[38] N. O. Eddy, H. Momoh-Yahaya, and E. E. Oguzie, "Theoretical and experimental studies on the corrosion inhibition potentials of some purines for aluminum in 0.1M HCl," *Journal of Advanced Research*, vol. 6, no. 2, pp. 203–217, 2015.

[39] A. K. Singh and M. A. Quraishi, "Effect of cefazolin on the corrosion of mild steel in HCl solution," *Corrosion Science*, vol. 52, no. 1, pp. 152–160, 2010.

[40] M. G. Tsoeunyane, M. E. Makhatha, and O. A. Arotiba, "Corrosion inhibition of mild steel by poly(butylene succinate)-L-histidine extended with 1,6-diisocynatohexane polymer composite in 1 M HCl," *International Journal of Corrosion*, vol. 2019, pp. 1–12, 2019.

[41] M. El Faydy, M. Galai, A. El Assyry et al., "Experimental investigation on the corrosion inhibition of carbon steel by 5-(chloromethyl)-8-quinolinol hydrochloride in hydrochloric acid solution," *Journal of Molecular Liquids*, vol. 219, pp. 396–404, 2016.

[42] M. Yadav, L. Gope, N. Kumari, and P. Yadav, "Corrosion inhibition performance of pyranopyrazole derivatives for mild steel in HCl solution: gravimetric, electrochemical and DFT studies," *Journal of Molecular Liquids*, vol. 216, pp. 78–86, 2016.

[43] H. Lgaz, R. Salghi, S. Jodeh, and B. Hammouti, "Effect of clozapine on inhibition of mild steel corrosion in 1.0 M HCl medium," *Journal of Molecular Liquids*, vol. 225, pp. 271–280, 2017.

[44] E. Elqars, M. Guennoun, N. Sqalli Houssini et al., "The adsorption performance of chicken excrement extract as corrosion inhibition of carbon steel in a 1 M HCl medium," *Journal of Bio- and Tribo-Corrosion*, vol. 7, no. 2, p. 77, 2021.

[45] H. M. Abd El-Lateef, "Corrosion inhibition characteristics of a novel salycilidene isatin hydrazine sodium sulfonate on carbon steel in HCl and a synergistic nickel ions additive: a combined experimental and theoretical perspective," *Applied Surface Science*, vol. 501, Article ID 144237, 2020.

[46] C. Verma, E. E. Ebenso, Y. Vishal, M. A. M.A.Quraishi, and " Dendrimers, "Dendrimers: a new class of corrosion inhibitors for mild steel in 1M HCl: experimental and quantum chemical studies," *Journal of Molecular Liquids*, vol. 224, pp. 1282–1293, 2016.

[47] A. Hamdy and N. S. El-Gendy, "Thermodynamic, adsorption and electrochemical studies for corrosion inhibition of carbon steel by henna extract in acid medium," *Egyptian Journal of Petroleum*, vol. 22, no. 1, pp. 17–25, 2013.

[48] E. Ech-chihbi, A. Nahlé, R. Salim et al., "Computational, MD simulation, SEM/EDX and experimental studies for understanding adsorption of benzimidazole derivatives as corrosion inhibitors in 1.0 M HCl solution," *Journal of Alloys and Compounds*, vol. 844, Article ID 155842, 2020.

[49] E. A. Noor and A. H. Al-Moubaraki, "Thermodynamic study of metal corrosion and inhibitor adsorption processes in mild steel/1-methyl-4[4′(-X)-styryl pyridinium iodides/hydrochloric acid systems," *Materials Chemistry and Physics*, vol. 110, no. 1, pp. 145–154, 2008.

[50] V. Srivastava, J. Haque, C. Verma et al., "Amino acid based imidazolium zwitterions as novel and green corrosion inhibitors for mild steel: experimental, DFT and MD studies," *Journal of Molecular Liquids*, vol. 244, pp. 340–352, 2017.

[51] Y. Koumya, R. Idouhli, A. Oukhrib et al., "Synthesis, electrochemical, thermodynamic, and quantum chemical investigations of amino cadalene as a corrosion inhibitor for stainless steel type 321 in sulfuric acid 1M," *International Journal of Electrochemistry*, vol. 2020, Article ID 5620530, 10 pages, 2020.

[52] A. K. Singh, S. Thakur, B. Pani, and G. Singh, "Green synthesis and corrosion inhibition study of 2-amino-N′-((thiophen-2-yl)methylene)benzohydrazide," *New Journal of Chemistry*, vol. 42, no. 3, pp. 2113–2124, 2018.

[53] H. Lgaz, R. Salghi, K. Subrahmanya Bhat, A. Chaouiki, Shubhalaxmi, and S. Jodeh, "Correlated experimental and theoretical study on inhibition behavior of novel quinoline derivatives for the corrosion of mild steel in hydrochloric acid solution," *Journal of Molecular Liquids*, vol. 244, pp. 154–168, 2017.

[54] J. Ding, B. Tang, M. Li et al., "Difference in the characteristics of the rust layers on carbon steel and their corrosion behavior in an acidic medium: limiting factors for cleaner pickling," *Journal of Cleaner Production*, vol. 142, pp. 2166–2176, 2017.

[55] Y. Guo, B. Xu, Y. Liu et al., "Corrosion inhibition properties of two imidazolium ionic liquids with hydrophilic tetrafluoroborate and hydrophobic hexafluorophosphate anions in acid medium," *Journal of Industrial and Engineering Chemistry*, vol. 56, pp. 234–247, 2017.

[56] A. K. Singh, B. Chugh, M. Singh et al., "Hydroxy phenyl hydrazides and their role as corrosion impeding agent: a detail experimental and theoretical study," *Journal of Molecular Liquids*, vol. 330, Article ID 115605, 2021.

[57] A. Elbarki, W. Guerrab, T. Laabaissi et al., "Chemical, electrochemical and theoretical studies of 3-methyl-5,5′-diphenylimidazolidine-2,4-dione as corrosion inhibitor for mild steel in HCl solution," *Chemical Data Collections*, vol. 28, Article ID 100454, 2020.

[58] N. Gunavathy and S. C. Murugavel, "Corrosion inhibition studies of mild steel in acid medium UsingMusa AcuminataFruit peel extract," *E-Journal of Chemistry*, vol. 9, no. 1, pp. 487–495, 2012.

[59] A. K. Singh and M. A. Quraishi, "The effect of some bisthiadiazole derivatives on the corrosion of mild steel in hydrochloric acid," *Corrosion Science*, vol. 52, no. 4, pp. 1373–1385, 2010.

[60] D. K. Lavanya, F. V. Priya, and D. P. Vijaya, "Green approach to corrosion inhibition of mild steel in hydrochloric acid by 1-[Morpholin-4-yl(thiophen-2-yl)methyl]thiourea," *Journal of Failure Analysis and Prevention*, vol. 20, no. 2, pp. 494–502, 2020.

[61] A. K. Singh, S. Mohapatra, and B. Pani, "Corrosion inhibition effect of Aloe vera gel: gravimetric and electrochemical study," *Journal of Industrial and Engineering Chemistry*, vol. 33, pp. 288–297, 2016.

[62] W. Emori, R.-H. Zhang, P. C. Okafor et al., "Adsorption and corrosion inhibition performance of multi-phytoconstituents from Dioscorea septemloba on carbon steel in acidic media: characterization, experimental and theoretical studies," *Colloids and Surfaces A: Physicochemical and Engineering Aspects*, vol. 590, Article ID 124534, 2020.

[63] M. Bouassiria, T. Laabaissi, F. Benhiba et al., "Corrosion inhibition effect of 5-(4-methylpiperazine)-methylquinoline-8-ol on carbon steel in molar acid medium," *Inorganic Chemistry Communications*, vol. 123, Article ID 108366, 2021.

[64] R. Hsissou, F. Benhiba, O. Dagdag et al., "Development and potential performance of prepolymer in corrosion inhibition for carbon steel in 1.0 M HCl: outlooks from experimental and computational investigations," *Journal of Colloid and Interface Science*, vol. 574, pp. 43–60, 2020.

[65] E. Aquino-Torres, R. L. Camacho-Mendoza, E. Gutierrez et al., "The influence of iodide in corrosion inhibition by organic compounds on carbon steel: theoretical and experimental studies," *Applied Surface Science*, vol. 514, Article ID 145928, 2020.

[66] A.-R. I. Mohammed, M. M. Solomon, K. Haruna, S. A. Umoren, and T. A. Saleh, "Evaluation of the corrosion inhibition efficacy of Cola acuminata extract for low carbon steel in simulated acid pickling environment," *Environmental Science and Pollution Research*, vol. 27, no. 27, pp. 34270–34288, 2020.

[67] B. Chugh, A. K. Singh, D. Poddar, S. Thakur, B. Pani, and P. Jain, "Relation of degree of substitution and metal protecting ability of cinnamaldehyde modified chitosan," *Carbohydrate Polymers*, vol. 234, Article ID 115945, 2020.

[68] M. Rbaa, P. Dohare, A. Berisha et al., "New Epoxy sugar based glucose derivatives as eco friendly corrosion inhibitors for the carbon steel in 1.0 M HCl: experimental and theoretical investigations," *Journal of Alloys and Compounds*, vol. 833, Article ID 154949, 2020.

[69] S. Cao, D. Liu, H. Ding, J. Wang, H. Lu, and J. Gui, "Corrosion inhibition effects of a novel ionic liquid with and without potassium iodide for carbon steel in 0.5 M HCl solution: an experimental study and theoretical calculation," *Journal of Molecular Liquids*, vol. 275, pp. 729–740, 2019.

[70] T. He, W. Emori, R.-H. Zhang, P. C. Okafor, M. Yang, and C.-R. Cheng, "Detailed characterization of Phellodendron chinense Schneid and its application in the corrosion inhibition of carbon steel in acidic media," *Bioelectrochemistry*, vol. 130, Article ID 107332, 2019.

[71] X. Zuo, W. Li, W. Luo et al., "Research of Lilium brownii leaves extract as a commendable and green inhibitor for X70 steel corrosion in hydrochloric acid," *Journal of Molecular Liquids*, vol. 321, Article ID 114914, 2021.

[72] S. Chen, H. Zhao, S. Chen, P. Wen, H. Wang, and W. Li, "Camphor leaves extract as a neoteric and environment friendly inhibitor for Q235 steel in HCl medium: combining experimental and theoretical researches," *Journal of Molecular Liquids*, vol. 312, Article ID 113433, 2020.

[73] S. Jayakumar, T. Nandakumar, M. Vadivel, C. Thinaharan, R. P. George, and J. Philip, "Corrosion inhibition of mild steel in 1 M HCl usingTamarindus indicaextract: electrochemical, surface and spectroscopic studies," *Journal of Adhesion Science and Technology*, vol. 34, no. 7, pp. 713–743, 2020.

[74] N. Dkhireche, M. Galai, M. Ouakki et al., "Electrochemical and theoretical study of newly quinoline derivatives as a corrosion inhibitors adsorption onmild steel in phosphoric acid media," *Inorganic Chemistry Communications*, vol. 121, Article ID 108222, 2020.

[75] M. Galai, M. Rbaa, M. Ouakki et al., "Chemically functionalized of 8-hydroxyquinoline derivatives as efficient corrosion inhibition for steel in 1.0 M HCl solution: experimental and theoretical studies," *Surfaces and Interfaces*, vol. 21, Article ID 100695, 2020.

[76] I. B. Obot, N. K. Ankah, A. A. Sorour, Z. M. Gasem, and K. Haruna, "8-Hydroxyquinoline as an alternative green and sustainable acidizing oilfield corrosion inhibitor," *Sustainable Materials and Technologies*, vol. 14, pp. 1–10, 2017.